NATIONAL ADVISORY COMMITTEE FOR AERONAUTICS

REPORT No. 687

c.3

EFFECT OF EXIT-SLOT POSITION AND OPENING ON THE AVAILABLE COOLING PRESSURE FOR N. A. C. A. NOSE-SLOT COWLINGS

By GEORGE W. STICKLE, IRVEN NAIMAN, and JOHN L. CRIGLER

1940

AERONAUTIC SYMBOLS

1. FUNDAMENTAL AND DERIVED UNITS

	Symbol	Metric		English	
		Unit	Abbreviation	Unit	Abbreviation
Length	l	meter	m	foot (or mile)	ft. (or mi.)
Time	t	second	s	second (or hour)	sec. (or hr.)
Force	F	weight of 1 kilogram	kg	weight of 1 pound	lb.
Power	P	horsepower (metric)		horsepower	hp.
Speed	V	kilometers per hour	k.p.h.	miles per hour	m.p.h.
		meters per second	m.p.s.	feet per second	f.p.s.

2. GENERAL SYMBOLS

W, Weight $= mg$

g, Standard acceleration of gravity $= 9.80665$ m/s² or 32.1740 ft./sec.²

m, Mass $= \dfrac{W}{g}$

I, Moment of inertia $= mk^2$. (Indicate axis of radius of gyration k by proper subscript.)

μ, Coefficient of viscosity

ν, Kinematic viscosity

ρ, Density (mass per unit volume)

Standard density of dry air, 0.12497 kg-m⁻⁴-s² at 15° C. and 760 mm; or 0.002378 lb.-ft.⁻⁴ sec.²

Specific weight of "standard" air, 1.2255 kg/m³ or 0.07651 lb./cu. ft.

3. AERODYNAMIC SYMBOLS

S, Area

S_w, Area of wing

G, Gap

b, Span

c, Chord

$\dfrac{b^2}{S}$, Aspect ratio

V, True air speed

q, Dynamic pressure $= \dfrac{1}{2}\rho V^2$

L, Lift, absolute coefficient $C_L = \dfrac{L}{qS}$

D, Drag, absolute coefficient $C_D = \dfrac{D}{qS}$

D_0, Profile drag, absolute coefficient $C_{D_0} = \dfrac{D_0}{qS}$

D_i, Induced drag, absolute coefficient $C_{D_i} = \dfrac{D_i}{qS}$

D_p, Parasite drag, absolute coefficient $C_{D_p} = \dfrac{D_p}{qS}$

C, Cross-wind force, absolute coefficient $C_C = \dfrac{C}{qS}$

R, Resultant force

i_w, Angle of setting of wings (relative to thrust line)

i_t, Angle of stabilizer setting (relative to thrust line)

Q, Resultant moment

Ω, Resultant angular velocity

$\rho\dfrac{Vl}{\mu}$, Reynolds Number, where l is a linear dimension (e.g., for a model airfoil 3 in. chord, 100 m.p.h. normal pressure at 15° C., the corresponding number is 234,000; or for a model of 10 cm chord, 40 m.p.s., the corresponding number is 274,000)

C_p, Center-of-pressure coefficient (ratio of distance of c.p. from leading edge to chord length)

α, Angle of attack

ϵ, Angle of downwash

α_0, Angle of attack, infinite aspect ratio

α_i, Angle of attack, induced

α_a, Angle of attack, absolute (measured from zero-lift position)

γ, Flight-path angle

REPORT No. 687

EFFECT OF EXIT-SLOT POSITION AND OPENING ON THE AVAILABLE COOLING PRESSURE FOR N. A. C. A. NOSE-SLOT COWLINGS

By GEORGE W. STICKLE, IRVEN NAIMAN, and JOHN L. CRIGLER

Langley Memorial Aeronautical Laboratory

I

NATIONAL ADVISORY COMMITTEE FOR AERONAUTICS

HEADQUARTERS, NAVY BUILDING, WASHINGTON, D. C.

LABORATORIES, LANGLEY FIELD, VA.

Created by act of Congress approved March 3, 1915, for the supervision and direction of the scientific study of the problems of flight (U. S. Code, Title 50, Sec. 151). Its membership was increased to 15 by act approved March 2, 1929. The members are appointed by the President, and serve as such without compensation.

VANNEVAR BUSH, Sc. D., *Chairman*,
  Washington, D. C.

GEORGE J. MEAD, Sc. D., *Vice Chairman*,
  West Hartford, Conn.

CHARLES G. ABBOT, Sc. D.,
  Secretary, Smithsonian Institution.

HENRY H. ARNOLD, Major General, United States Army,
  Chief of Air Corps, War Department.

GEORGE H. BRETT, Brigadier General, United States Army,
  Chief Matériel Division, Air Corps, Wright Field, Dayton,
  Ohio.

LYMAN J. BRIGGS, Ph. D.,
  Director, National Bureau of Standards.

ROBERT E. DOHERTY, M. S.,
  Pittsburgh, Pa.

CLINTON M. HESTER, A. B., LL. B.,
  Administrator, Civil Aeronautics Authority.

ROBERT H. HINCKLEY, A. B.,
  Chairman, Civil Aeronautics Authority.

JEROME C. HUNSAKER, Sc. D.,
  Cambridge, Mass.

SYDNEY M. KRAUS, Captain, United States Navy,
  Bureau of Aeronautics, Navy Department.

FRANCIS W. REICHELDERFER, Sc. D.,
  Chief, United States Weather Bureau.

JOHN H. TOWERS, Rear Admiral, United States Navy,
  Chief, Bureau of Aeronautics, Navy Department.

EDWARD WARNER, Sc. D.,
  Washington, D. C.

ORVILLE WRIGHT, Sc. D.,
  Dayton, Ohio.

GEORGE W. LEWIS, *Director of Aeronautical Research*   S. PAUL JOHNSTON, *Coordinator of Research*

JOHN F. VICTORY, *Secretary*

HENRY J. E. REID, *Engineer in Charge, Langley Memorial Aeronautical Laboratory, Langley Field, Va.*

JOHN J. IDE, *Technical Assistant in Europe, Paris, France*

TECHNICAL COMMITTEES

AERODYNAMICS
POWER PLANTS FOR AIRCRAFT
AIRCRAFT MATERIALS

AIRCRAFT STRUCTURES
AIRCRAFT ACCIDENTS
INVENTIONS AND DESIGNS

Coordination of Research Needs of Military and Civil Aviation

Preparation of Research Programs

Allocation of Problems

Prevention of Duplication

Consideration of Inventions

LANGLEY MEMORIAL AERONAUTICAL LABORATORY

LANGLEY FIELD, VA.

Unified conduct, for all agencies, of scientific research on the fundamental problems of flight.

OFFICE OF AERONAUTICAL INTELLIGENCE

WASHINGTON, D. C.

Collection, classification, compilation, and dissemination of scientific and technical information on aeronautics.

4-1-40

REPORT No. 687

EFFECT OF EXIT-SLOT POSITION AND OPENING ON THE AVAILABLE COOLING PRESSURE FOR N. A. C. A. NOSE-SLOT COWLINGS

By George W. Stickle, Irven Naiman, and John L. Crigler

SUMMARY

An investigation of full-scale nose-slot cowlings has been conducted in the N. A. C. A. 20-foot wind tunnel to furnish information on the pressure drop available for cooling. Engine conductances from 0 to 0.12 and exit-slot conductances from 0 to 0.30 were covered. Two basic nose shapes were tested to determine the effect of the radius of curvature of the nose contour; the nose shape with the smaller radius of curvature gave the higher pressure drop across the engine. The best axial location of the slot for low-speed operation was found to be in the region of maximum negative pressure for the basic shape for the particular operating condition. The effect of the propeller operating condition on the available cooling pressure is shown. The maximum pressure drop $\Delta p/q$ obtained for the high-speed condition with an engine conductance equivalent to that of a modern double-row radial engine and a propeller with good blade sections near the hub is 1.45 and, for the take-off condition, is 3.75; for a propeller with a round blade shank, the values are 1.23 and 1.65, respectively.

INTRODUCTION

The N. A. C. A. nose-slot cowling, first discussed in reference 1, is characterized by the location of the exit slot near the nose, making it possible to locate the slot in a high-velocity, low-pressure region. The limitations of the set-up prevented the investigation reported in reference 1 from covering a sufficiently wide range of engine and exit-slot conductances to make the results easily applicable to design. The investigation has been extended to include the effects of location and size of exit slot, of engine conductance, and of the radius of curvature of the basic nose shape. The results show the effects of exhausting the air in the nose section of the cowling and are applicable to any design in which the exit slot is so located. The most important result presented herein is the pressure drop available for cooling obtained with several propellers under all operating conditions.
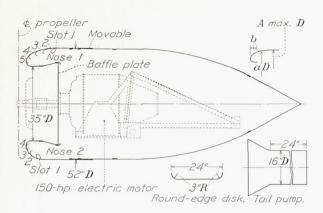
APPARATUS

The investigation was conducted in the N. A. C. A. 20-foot wind tunnel which, with its standard equip-

FIGURE 1.—The set-up mounted on the balance. Nose 1; slot 3; opening, 3 inches; propeller E.

ment, is described in reference 2. Figure 1 shows the general arrangement of the set-up on the tunnel balance. A line drawing of the set-up is given in figure 24.

1

Slot locations		
	b/A Ordinate	
Slot	Nose 1	Nose 2
1	0.267	0.106
2	.199	.046
3	.103	.011
4	.039	0
5	0	-----

Basic-shape ordinates			
		a/A	
Station	b/A	Nose 1	Nose 2
1	0	0.769	0.769
2	.01	.822	.862
3	.02	.847	.896
4	.04	.884	.937
5	.06	.910	.965
6	.08	.930	.984
7	.10	.947	.996
8	.12	.959	1.000
9	.14	.969	-----
10	.16	.978	-----
11	.19	.987	-----
12	.22	.994	-----
13	.25	.998	-----
14	.28	1.000	-----

FIGURE 2.—Layout of the test arrangement.

A baffle plate was constructed as a shutter with four stops, controlled from the balance house, that simulated engine conductances of 0, 0.037, 0.078, and 0.116. The propeller was driven by a 150-horsepower, three-phase, wound-rotor induction motor mounted in the nacelle. The speed and the power output of the motor were controlled by resistance in the rotor circuit. The cooling in the front of the cowling has been measured for several conditions of engine conductance and propeller operation. This information will be the subject of a separate report. Pressures over the nose, inside the exit slot, and across the engine baffle were photographically recorded on a multiple-tube manometer.

It has been shown (reference 3) that a well-designed nose section must have a change in angular direction of approximately 90° in order to meet the local air flow and that the distance in which this angular change is made sets the lower limit of the increase in velocity over the nose. This distance may be called the length of the nose section. The length of the nose section for nose 1 was 14½ inches and for nose 2 was 6¼ inches. Each nose was designed to give as low a maximum velocity as possible for the given length. The slots were built into the noses as shown in figure 2 and were opened by an axial movement of the after part of the nose. The slot opening given in the results refers to the distance of axial movement and not to the width of the slot. The distance between the cowling and the propeller has been found to affect the pressure available for ground cooling (reference 4) and was therefore maintained constant throughout the tests.

The propellers used for this investigation are shown in figure 3. Propeller C is a three-blade propeller with Navy plan form 5868–11, diameter of 9 feet 10 inches, and round blade shanks. Propeller D is a similar two-blade propeller. Propeller E is a three-blade propeller with Navy plan form 3790, diameter of 9 feet, and airfoil sections near the blade shanks.

SYMBOLS

A_2 area of exit slot.

C orifice coefficient $(K_2 F / A_2)$.

F projected frontal area of nacelle.

η_0 net efficiency of propeller-nacelle unit with exit closed (RV/P).

η_n net efficiency of propeller-nacelle unit with air flowing.

η_p pump efficiency of cowling.

K conductance of engine or baffle plate.

K_2 conductance of exit slot.

P power supplied to propeller.

P_c power disk-loading coefficient (P/qSV).

Δp pressure drop across engine or baffle plate $(p_f - p_r)$.

ΔP pressure difference available for pumping air.

p_f pressure in front of engine or baffle plate.

p_r pressure in rear of engine or baffle plate.

q dynamic pressure of air stream $(\frac{1}{2}\rho V^2)$.

Q volume of air flowing through cowling per second.

R net thrust of propeller-nacelle unit.

ρ mass density of air.

S disk area of propeller.

V velocity of air stream.

METHODS

One advantage of the nose-slot cowling is its capability of developing a large pressure drop across the baffle for low-speed operation. This low-speed condition is characterized by a large propeller slipstream contraction and is entirely different from the condition of propeller removed. Consequently, this investigation was confined to tests with a propeller. A constant blade-angle setting of 20° at 75 percent of the radius (0.75R) was used throughout the tests. This setting
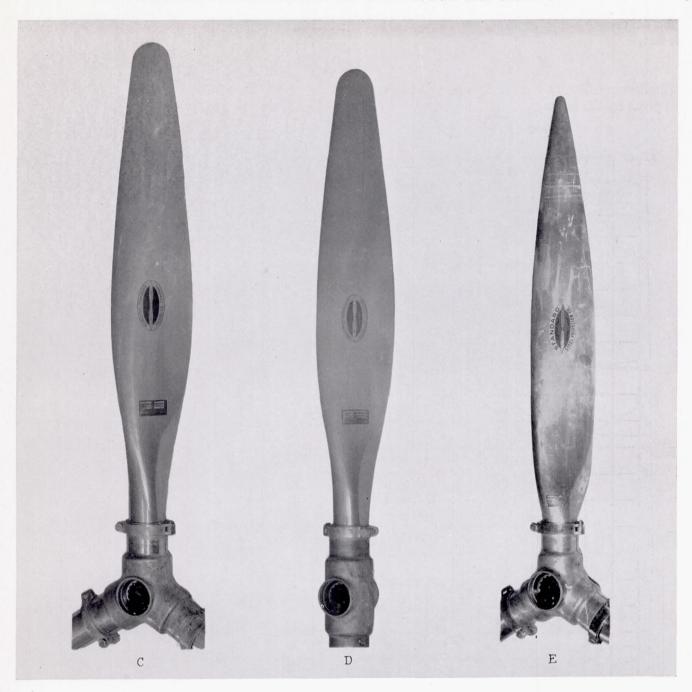
FIGURE 3.—The propellers used in this investigation.

is representative of the low-speed operating conditions as encountered in present-day practice. Comparisons are made for constant disk loading, defined as

$$P_c = \frac{P}{qSV} \tag{1}$$

This quantity for a given propeller and blade-angle setting is a measure of the contraction of the propeller slipstream (reference 5). Equal values of P_c (or of $1/\sqrt[3]{P_c}$, the form used) essentially represent geometrically identical flow pictures.

The net efficiency is defined as

$$\eta_n = \frac{RV}{P} \tag{2}$$

where R is the net force of the test unit as recorded on the balance. The net efficiency with the nose slots all closed is η_0.

The conductance K of the baffle plate was determined by the formula, from reference 5,

$$K = \frac{Q}{FV\sqrt{\dfrac{\Delta p}{q}}}$$

The volume of air Q was obtained from survey measurements in the tail pump shown in figure 2. The area of the exit slot A_2 multiplied by an effective-area coefficient C and divided by the frontal area of the

engine or the cowling F gives the conductance of the exit slot,

$$K_2 = \frac{CA_2}{F} \tag{3}$$

The flow equation of the air through the cowling is then given by the formula

$$\frac{\Delta P}{\Delta p} = 1 + \left(\frac{K}{K_2}\right)^2 \tag{4}$$

The pump efficiency with the propeller operating is given in reference 5 as

$$\eta_p = \frac{KF}{SP_c} \frac{\left(\frac{\Delta p}{q}\right)^{3/2}}{\eta_0 - \eta_n}$$

RESULTS

The experimental results are presented in a condensed

(a) $K=0$.   (b) $K=0.037$.   (c) $K=0.078$.   (d) $K=0.116$.
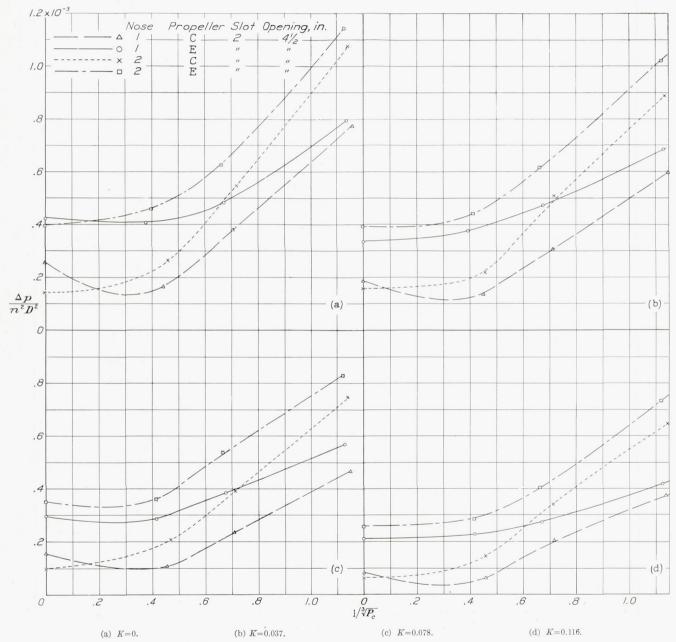
FIGURE 4.—Curves of $\frac{\Delta p}{n^2 D^2}$ against $1/\sqrt[3]{P_c}$ for one slot on each nose for propellers C and E set 20° at 0.75R.
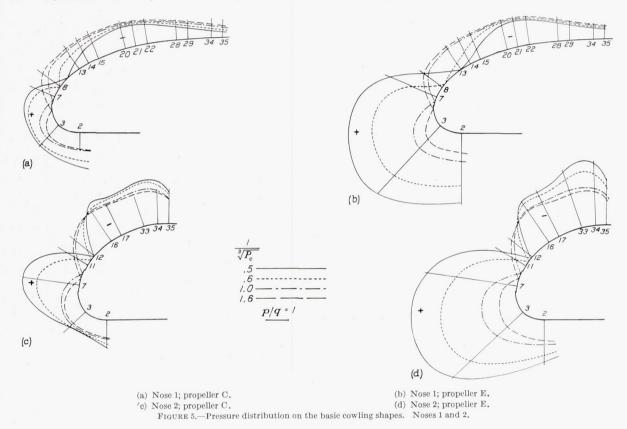
where ΔP is equal to the difference between the total pressure in front of the engine and the static pressure at the location of the exit slot for zero engine conductance.

The change in propeller disk loading was obtained by varying the air speed of the tunnel. The tunnel entrance cone was blocked off with canvas to obtain the static condition.

form in table I. The table is given in four divisions, each division presenting one engine, or baffle-plate, conductance. The grouping in each division is on the basis of the propeller used. The columns are arranged in five groups representing four conditions of propeller operation: $1/\sqrt[3]{P_c}=0$, the static condition; $1/\sqrt[3]{P_c}=0.5$ and 0.6, the take-off condition; $1/\sqrt[3]{P_c}=1.0$, the climbing condition; and $1/\sqrt[3]{P_c}=1.6$, the high-speed condition.

The pressures available across the baffles are given in the form $\Delta p/n^2 D^2$ for the static condition and in the form $\Delta p/q$ for the other operating conditions. The column p_r/q is given to show the effectiveness of the exit slot in producing a suction behind the baffle plate. Figure 4, which presents the variation of $\Delta p/n^2 D^2$ with disk-loading coefficient $1/\sqrt[3]{P_c}$ as obtained for the test conditions, is given to correlate the data in table I for the static condition with those for the take-off condition. The figure should not be used as a basis for computing the Δp obtainable for the climbing and the high-speed conditions. Values of the net and the pump efficiencies are included in table I for purposes of comparison but they should not be used as

$1/\sqrt[3]{P_c}$, slot 3 is much the poorer and, in the static condition, gives a reverse flow through the baffle plate.

Figure 6 presents all the data for the high-speed condition, $1/\sqrt[3]{P_c}=1.6$, plotted on one curve. In the ratio $\Delta p/\Delta P$, Δp is the pressure drop across the baffle plate at any engine conductance and ΔP is the pressure drop across the baffles for zero engine conductance. The ratio of these pressure drops is plotted as a function of the engine conductance K divided by the ratio of the area of the exit slot to the frontal area of the engine. The theoretical relationship of these quantities is given in equations (3) and (4). If the effective-area coefficient is unity, then equation (4) gives the theoretical relationship. The experimental curve may be used for

(a) Nose 1; propeller C.
(b) Nose 1; propeller E.
(c) Nose 2; propeller C.
(d) Nose 2; propeller E.

FIGURE 5.—Pressure distribution on the basic cowling shapes. Noses 1 and 2.

absolute values because a critical flow over the rear portion of the nacelle makes them generally too high.

Figure 5 gives the pressure distribution on the basic shapes of the two noses with propellers C and E. The smooth low-pressure distribution on nose 1 indicates that the shape is almost optimum for the given length of nose section. Nose 2, with the smaller radius of curvature, shows a considerably larger negative pressure. The point of zero pressure moves forward as the propeller disk loading is decreased, showing why a nose slot that gives a high pressure drop for cooling in the level-flight or the climb condition may be very poor for the ground or the take-off condition if the slot is located too far forward. For example, a comparison of the pressures for slots 2 and 3 on nose 2 with propeller C (table I) shows that, at $1/\sqrt[3]{P_c}=1.6$, the two slots give equal pressure for cooling; but, for lower values of

computing the area A_2 necessary to produce a given pressure drop across the baffles for a given engine conductance and slot location. The curve of effective-area coefficient shows that, as the ratio of $K/(A_2/F)$ becomes small, an increase of the area of the slot is offset to a large extent by the decreasing coefficient.

Figures 7 and 8 show how $\Delta p/q$ varies with slot opening at the take-off condition, $1/\sqrt[3]{P_c}=0.5$, for the two nose shapes tested. The superiority of propeller E, which has airfoil sections near the hub, is clearly demonstrated. Slot 3 with nose 1 and slot 2 with nose 2 give the highest $\Delta p/q$ for this flight condition. As would be expected from a consideration of the available ΔP, nose 2 produces greater pressure drops than nose 1.

Figures 9 and 10, giving the pressure distributions for nose 1, slot 2, and a 4½-inch opening with propellers C and E, respectively, show the effect of propeller oper-
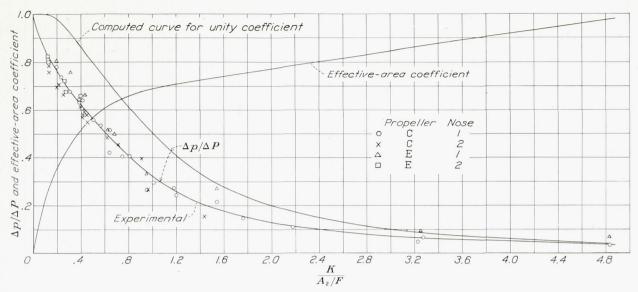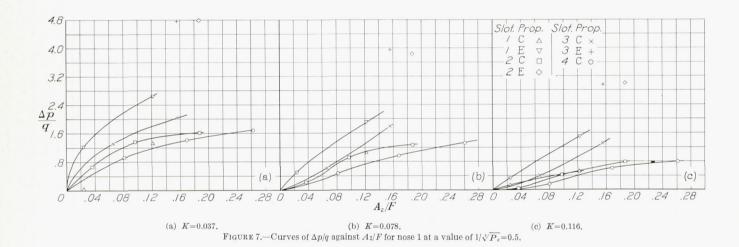
FIGURE 6.—Comparison of the experimental and the theoretical variation of $\Delta p/\Delta P$ with $K/(A_2/F)$. $1/\sqrt[3]{P_c}=1.6$.

(a) $K=0.037$.   (b) $K=0.078$.   (c) $K=0.116$.

FIGURE 7.—Curves of $\Delta p/q$ against A_2/F for nose 1 at a value of $1/\sqrt[3]{P_c}=0.5$.

(a) $K=0.037$.   (b) $K=0.078$.   (c) $K=0.116$.
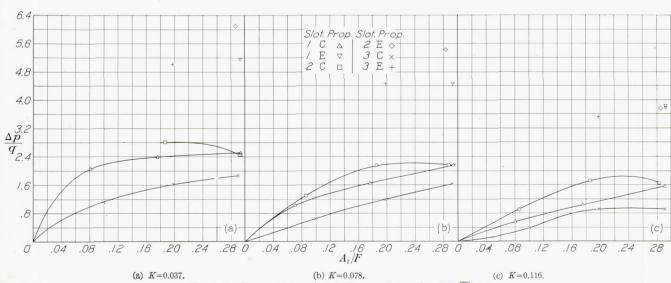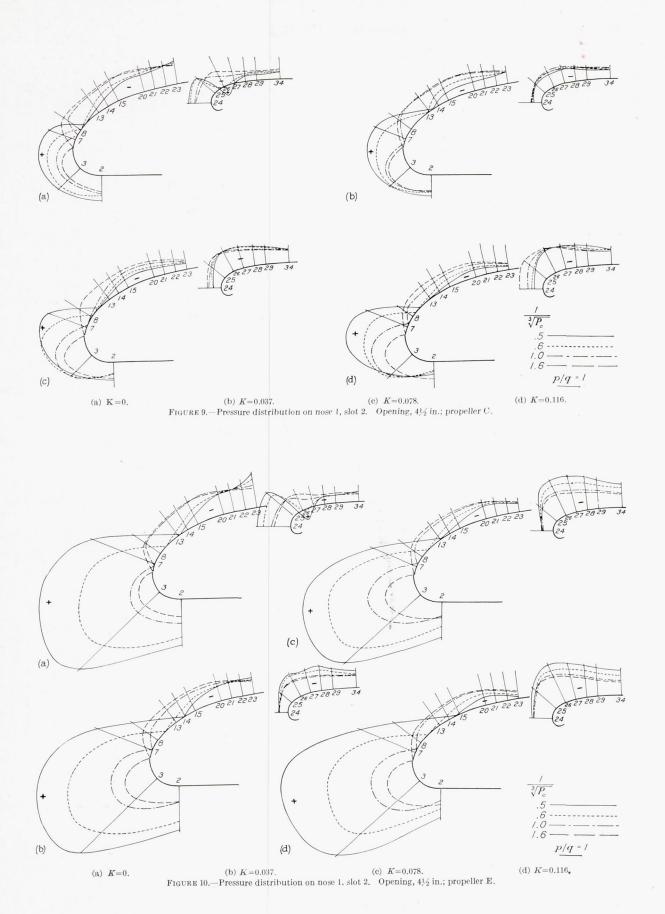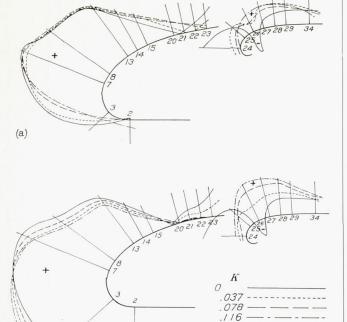
FIGURE 8.—Curves of $\Delta p/q$ against A_2/F for nose 2 at a value of $1/\sqrt[3]{P}=0.5$.

(a) K=0.   (b) K=0.037.   (c) K=0.078.   (d) K=0.116.

FIGURE 9.—Pressure distribution on nose 1, slot 2.   Opening, 4½ in.; propeller C.

(a) K=0.   (b) K=0.037.   (c) K=0.078.   (d) K=0.116.

FIGURE 10.—Pressure distribution on nose 1, slot 2.   Opening, 4½ in.; propeller E.

(a)

(b)

$$K$$
$$0 \quad \text{————————}$$
$$.037 \quad \text{- - - - - - - -}$$
$$.078 \quad \text{— — — —}$$
$$.116 \quad \text{—·——·——}$$

$$10^4 \times \frac{p}{n^2 D^2} = 1$$

(a) Propeller C.   (b) Propeller E.

FIGURE 11.—Pressure distribution on nose 1, slot 2. Opening 4½ in.; $1/\sqrt{P_c}=0$.

ating condition and engine conductance on the pressure distribution. Figure 11, giving the pressure distributions for nose 1, slot 2, and a 4½-inch opening for the static condition, is presented in the form of p/n^2D^2 for comparison of the location of zero pressure with figures 9 and 10. A consideration of the point of zero pressure indicates that, for the slot to be in the negative-pressure region, the slot location must be farther back for the ground condition than for any flight condition. A plot of the pressure distribution for nose 2, slot 2,

and propeller C at a value of $1/\sqrt[3]{P_c}=1.6$ is given in figure 12 and shows the pressure-distribution change with slot opening for all conductances tested.
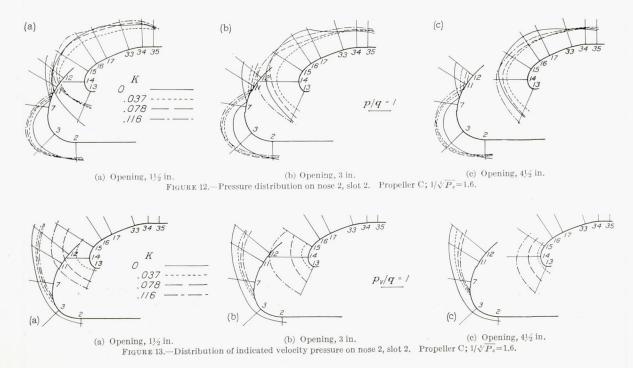
Figure 13 gives the distribution of indicated velocity pressure, $p_T/q-p/q=p_V/q$, around the nose of the cowling, obtained by deducting the p/q on the pressure-distribution plots from unity for the p_V/q ahead of the slot and from p_T/q for the p_V/q inside the slot. This plot should be used only for comparative purposes because the total pressures used in its determination are approximate.

DISCUSSION OF RESULTS

The values of $\Delta p/q$ in table I show a marked change with propeller operating condition. If the slot location is such that the $\Delta p/q$ on the ground is large, it is favorable for all operating conditions. Variation of $\Delta p/q$ with slot location, however, is less marked for the high-speed condition.

For the ground condition, $1/\sqrt[3]{P_c}=0$, propeller E gives a greater pressure drop than propellers C and D. This greater pressure drop is due, first, to the airfoil sections of the blade shanks of propeller E and, second, to the ratio of the cowling opening to the propeller diameter, which is 0.324 for propeller E and 0.296 for propellers C and D. It was shown in reference 4 that, for this range of values, the available pressure rapidly increased as the ratio increased. The results for the ground condition must be interpreted in accordance with reference 4 because anything that affects the total pressure in front of the engine produces a like effect in the pressure drop across the engine.

As would be expected from a consideration of figure 5, nose 2 gives a larger available pressure than nose 1. It is possible that the effect of decreasing the radius of cur-

(a)   (b)   (c)

$$K$$
$$0 \quad \text{————}$$
$$.037 \quad \text{- - - -}$$
$$.078 \quad \text{— — —}$$
$$.116 \quad \text{—·——}$$

$$p/q = 1$$

(a) Opening, 1½ in.   (b) Opening, 3 in.   (c) Opening, 4½ in.

FIGURE 12.—Pressure distribution on nose 2, slot 2. Propeller C; $1/\sqrt[3]{P_c}=1.6$.

(a)   (b)   (c)

$$K$$
$$0 \quad \text{————}$$
$$.037 \quad \text{- - - -}$$
$$.078 \quad \text{— — —}$$
$$.116 \quad \text{—·——}$$

$$p_V/q = 1$$

(a) Opening, 1½ in.   (b) Opening, 3 in.   (c) Opening, 4½ in.

FIGURE 13.—Distribution of indicated velocity pressure on nose 2, slot 2. Propeller C; $1/\sqrt[3]{P_c}=1.6$.

vature can be used to produce larger pressures than those obtained on nose 2. If a nose shape is designed to produce too large a negative pressure, however, almost any break in the contour may cause a breakdown in the flow and the consequent loss of available cooling pressure associated with extremely high drag. In order to obtain good cowling performance at high speeds, a small radius of curvature should not be resorted to because the basic drag will increase too much. The nose shapes tested in this investigation are useful for present-day cowling design and will give almost equal performance for high speeds up to 350 miles per hour. Beyond that speed, it is better to use nose 1 to insure freedom from a local compressibility burble.

The axial, or angular, location of the slot is not very critical for the nose shapes tried. When the cooling pressure for low-speed operation is considered, it is imperative that the slot location be in a negative pressure region. This necessity eliminates all slot locations ahead of the position of zero pressure on the basic-shape pressure distribution; for example, slots 4 and 5 on nose 1 and slots 3 and 4 on nose 2 are thus eliminated for low speed. When pump efficiency for the high-speed condition is considered, all slot locations will apparently give almost equal efficiency if, as in the present investigation, the closed slot is designed to fit into the basic shape. This result indicates that a variable-area single slot may be equally as good as separate slots for high- and low-speed operation.

A comparison of the pressure distributions in figures 9 and 10 shows the same trends with a change in propeller operating condition as are shown in figure 5 for the basic-shape pressure distribution. Figure 12 shows that a similar shift in the pressure distribution is obtained by increasing the baffle conductance at a constant propeller operating condition. Figure 13 interprets the pressure distribution in terms of velocity distribution. The total pressure over the outside of the cowling is nearly equal to the dynamic pressure of the free air stream for this operating condition and q was therefore used as the total pressure. The total pressure inside the cowling is equal to that behind the baffle plate, if no losses are experienced in the return ducts and the turns. The value of p_r was therefore used as a basis for computing velocity inside the slot. It is interesting to note how the velocity distribution inside the slot changes with the slot opening. For the 1½-inch slot, the constant increase in velocity up to the slot exit gives a very desirable condition of flow. For the 3-inch opening and the two lower engine conductances, the velocity also increases up to the exit. For the largest conductance, however, the highest velocity is obtained at orifice 14 (fig. 13) showing the beginning of a bad condition. For the 4½-inch opening, the lowest velocity is obtained at the slot exit, or orifice 15. Here the importance of having a large radius of curvature of the inner lip for large exit openings is apparent.

The exit passage may be compared with a pipe having an approximately 180° bend.

The increase in friction loss per unit length of bend divided by the friction loss per unit length of straight pipe is given by Betz (reference 6) as

$$\zeta \propto \text{constant} + \left(\frac{d}{r}\right)^{3.5}$$

where d is the pipe diameter and r is the mean radius of curvature of the bend.

The radius of bend r is analogous to the radius of the inside lip of the exit slot and the diameter is analogous to the width of the exit opening. As the opening is increased and the radius of bend remains constant, it can be seen that the loss becomes rapidly greater. This fact shows the importance of having as large a radius of curvature as space limitations permit for the inside surface of the exit slot. If this bend is too sharp, there is danger of a breakdown of flow with a complete stall of the cowling back of the exit slot and a consequent high drag and small cooling pressure. The radius of bend is a function of the slot opening. If the radius of bend is suitable for maximum slot opening, it will be equally good for all smaller openings. In the present investigation, no breakdown of flow occurred over the inside lip of the cowling but, in an unpublished flight test, this condition occurred, giving very rough operation of the airplane combined with a large increase in drag. The test results do indicate that such a condition is possible since, in many instances with large exit openings, the maximum negative pressure on the entire cowling was on the inside lip of the slot. (Note figs. 9 and 11 for an engine conductance of 0.116 and a 4½-inch slot opening.) The foregoing discussion indicates that it may be necessary to resort to guide vanes or multiple slots in order to realize the full benefit of large exit conductances.

CONCLUSIONS

1. The maximum values of $\Delta p/q$, taken from table I, are tabulated for the two nose shapes and the two propellers used in this investigation.

Cowling and propeller designation					Conductance, K				Conductance, K			
Nose	Slot	Slot opening (in.)	Propeller	A_2/F	0	0.037	0.078	0.116	0	0.037	0.078	0.116
					Take-off $1/\sqrt[3]{P_c}=0.5$				Take-off $1/\sqrt[3]{P_c}=0.6$			
1	3	3	C	0.156	2.60	2.05	1.80	1.32	2.45	2.00	1.62	1.15
1	3	3	E	.156	5.40	4.78	3.97	2.97	4.15	3.67	3.01	2.28
2	2	4½	C	.286	2.90	2.47	2.16	1.65	2.77	2.46	2.00	1.67
2	2	4½	E	.286	6.63	6.10	5.23	3.75	4.83	4.63	4.07	2.97
					Climb $1/\sqrt[3]{P_c}=1.0$				High Speed $1/\sqrt[3]{P_c}=1.6$			
1	3	3	C	0.156	1.98	1.48	1.13	0.82	1.86	1.37	1.04	0.75
1	3	3	E	.156	2.48	2.08	1.67	1.17			1.28	.87
2	2	4½	C	.286	2.40	2.05	1.65	1.49	2.17	1.64	1.45	1.23
2	2	4½	E	.286	3.02	2.69	2.19	1.96	2.41	1.93	1.64	1.45

From this table it can be seen that:

(a) Cooling pressures of several times the dynamic pressure of the air stream can be obtained for the low-speed flight conditions, not only with small engine conductances but also with large conductances corresponding to modern double-row radial engines.

(b) The data of the table confirm the earlier conclusion that the cooling pressure for low air speed is greatly dependent on the propeller blade section near the hub.

(c) There exists an optimum radius of curvature of the nose section of the cowling. If the radius is too large, small cooling pressures result; if the radius is too small, a condition is reached in which breakdown occurs, at least for the largest slot openings. For the ordinary present-day speed range, nose 2 is probably near the optimum radius.

2. For maximum ground cooling, it is important to locate the slot in the region of maximum negative pressure for the static condition.

3. It is important to have a relatively large radius on the inner lip of the slot, particularly when large engine conductances and exit slots are used.

4. For the condition of high-speed flight, the location of the exit slot is not critical in regard to either pressure drop or efficiency.

5. Greater care in streamlining the nacelle of a nose-slot cowling is required because of the more forward location of the exit slot as compared with that of the conventional N. A. C. A. cowling.

LANGLEY MEMORIAL AERONAUTICAL LABORATORY,
    NATIONAL ADVISORY COMMITTEE FOR AERONAUTICS,
      LANGLEY FIELD, VA., *January 18, 1939.*

REFERENCES

1. Theodorsen, Theodore, Brevoort, M. J., Stickle, George W., and Gough, M. N.: Full-Scale Tests of a New Type N. A. C. A. Nose-Slot Cowling. T. R. No. 595, N. A. C. A., 1937.
2. Weick, Fred E., and Wood, Donald H.: The Twenty-Foot Propeller Research Tunnel of the National Advisory Committee for Aeronautics. T. R. No. 300, N. A. C. A., 1928.
3. Stickle, George W.: Design of N. A. C. A. Cowlings for Radial Air-Cooled Engines. T. R. No. 662, N. A. C. A., 1939.
4. Stickle, George W., and Joyner, Upshur T.: The Pressure Available for Ground Cooling in Front of the Cowling of Air-Cooled Airplane Engines. T N No. 673, N. A. C. A., 1938.
5. Theodorsen, Theodore, Brevoort, M. J., and Stickle, George W.: Full-Scale Tests of N. A. C. A. Cowlings. T. R. No. 592, N. A. C. A., 1937.
6. Betz, A.: Mechanik unelasticher Flüssigkeiten. 1. Bd., 2.Abschn. V des Ingenieurs Taschenbuch, 26. Auflage, herausg. vom Akademischen Verein Hütte, Wilhelm Ernst & Sohn (Berlin), 1931, S. 379.

TABLE I.—CONDENSED EXPERIMENTAL RESULTS

Nose	Slot	Slot opening (in.)	Propeller	A_2/F	$\frac{1}{\sqrt[3]{P_c}}=0$		$\frac{1}{\sqrt[3]{P_c}}=0.5$				$\frac{1}{\sqrt[3]{P_c}}=0.6$				$\frac{1}{\sqrt[3]{P_c}}=1.0$				$\frac{1}{\sqrt[3]{P_c}}=1.6$			
					$\frac{\Delta p}{n^2D^2}\times1000$	$\frac{p_r}{n^2D^2}\times1000$	$\frac{\Delta p}{q}$	$\frac{p_r}{q}$	η_n	η_p	$\frac{\Delta p}{q}$	$\frac{p_r}{q}$	η_n	η_p	$\frac{\Delta p}{q}$	$\frac{p_r}{q}$	η_n	η_p	$\frac{\Delta p}{q}$	$\frac{p_r}{q}$	η_n	η_p
CONDUCTANCE=0																						
1			C						ª0.460				ª0.513				ª0.648				ª0.603	
1	1	1½	C	0.024			1.23	−0.16	.453		1.29	−0.25	.516		1.24	−0.39	.648		1.21	−0.38	.603	
1	1	3½	C	.122			1.97	−.16	.455		1.69	−.25	.518		1.35	−.43	.646		1.28	−.45	.596	
1	1	4½	C	.182	0.177	−0.064																
1	2	1½	C	.036	.219	−.065	2.06	−.72	.455		1.86	−.72	.511		1.59	−.68	.642		1.48	−.63	.565	
1	2	3	C	.097	.258	−.080	1.93	−.72	.455		1.87	−.80	.512		1.67	−.74	.635		1.57	−.69	.562	
1	2	4½	C	.187	.260	−.081	1.98	−.85	.460		1.92	−.82	.516		1.69	−.73	.642		1.54	−.69	.560	
1	3	1½	C	.066			2.42	−1.06	.453		2.25	−1.05	.514		1.95	−1.02	.639		1.83	−.97	.563	
1	3	3	C	.156			2.60	−1.30	.450		2.45	−1.22	.508		1.98	−1.06	.630		1.86	−1.01	.548	
1	3	4½	C	b.253	.195	−.054																
1	4	1½	C	.081			1.74	−.46	.457		1.84	−.58	.519		1.94	−.96	.650		1.94	−1.11	.552	
1	4	3	C	b.168			1.88	−.70	.454		1.91	−.85	.511		1.98	−1.07	.636		1.93	−1.08	.534	
1	4	4½	C	b.262			2.03	−.66	.459		2.00	−.83	.512		1.93	−1.02	.630		1.90	−1.04	.533	
1		(c)	C						ª.453				ª.512				ª.640				ª.565	
2			C						ª.453				ª.511				ª.616				ª.558	
2	1	1½	C	.081			3.46	−2.27	.449		3.00	−1.82	.509		2.41	−1.46	.640		2.06	−1.19	.525	
2	1	3	C	.176			3.25	−2.01	.456		2.88	−1.75	.510		2.29	−1.36	.632		2.04	−1.18	.532	
2	1	4½	C	.296	.296	−.145	3.36	−1.98	.451		2.94	−1.75	.510		2.24	−1.33	.630		1.97	−1.14	.525	
2	2	1½	C	.086					.452				.510		2.50	−1.60	.640		2.33	−1.46	.520	
2	2	3	C	.186			3.29	−1.65	.447		3.02	−1.67	.505		2.50	−1.54	.631		2.31	−1.44	.522	
2	2	4½	C	b.286	.141	−.039	2.90	−1.59	.452		2.77	−1.58	.509		2.40	−1.44	.628		2.17	−1.30	.504	
2	3	1½	C	.100			1.68	−.40	.455		1.84	−.78	.512		2.04	−1.12	.640		2.13	−1.29	.548	
2	3	3	C	b.198			1.88	−.68	.450		2.02	−.89	.509		2.18	−1.23	.630		2.18	−1.31	.524	
2	3	4½	C	b.292	.030	.085	2.02	−.64	.452		2.06	−.90	.510		2.14	−1.21	.631		2.16	−1.26	.510	
1	3	3	D	.156			2.85	−1.43	.437		2.53	−1.34	.498		2.06	−1.12	.620			−.99	.567	
1			E						ª.441				ª.502				ª.632				ª.573	
1	1	1½	E	.024			2.80	−.40	.448		2.25	−.41	.518		1.60	−.42	.640		1.38	−.43	.600	
1	1	3½	E	.122			3.12	−.61	.439		2.46	−.51	.502		1.74	−.47	.630		1.36	−.43	.554	
1	1	4½	E	.182	.367	−.071																
1	2	1½	E	.036	.382	−.077																
1	2	3	E	.097	.427	−.096																
1	2	4½	E	.187	.424	−.103	4.90	−1.36	.441		3.72	−1.14	.500		2.13	−.83	.622		1.73	−.73	.498	
1	3	3	E	.156			5.40	−1.64	.438		4.15	−1.42	.493		2.48	−1.18	.616				.461	
1	3	4½	E	b.253	.360	−.096																
1	3	d4½	E	b.253	.363	−.091																
1		(c)	E						ª.440				ª.497				ª.617				ª.504	
2			E						ª.440				ª.499				ª.624				ª.504	
2	1	4½	E	.296	.455	−.156			.435		4.59	−1.97	.492		2.73	−1.44	.606		2.18	−1.20	.450	
2	1	d4½	E	.296	.411	−.163	6.26	−2.60	.449		4.80	−2.18	.510		2.80	−1.46	.630		2.22	−1.18	.470	
2	2	4½	E	b.286	.399	−.079	6.63	−2.25	.434		4.83	−2.00	.493		3.02	−1.62	.606		2.41	−1.43	.432	
2	3	3	E	b.198			5.60	−1.12	.436		4.40	−1.25	.492		2.91	−1.41	.607		2.35	−1.39	.438	
CONDUCTANCE=0.037																						
1	1	1½	C	0.024			0.04	0.96	0.459	0.01	0.34	0.77	0.517		0.32	0.57	0.650		0.26	0.58	0.606	
1	1	3½	C	.122			1.34	.29	.455	.27	1.17	.15	.517		.94	−.10	.640	0.80	.87	−.20	.570	0.71
1	1	4½	C	.182	0.162	−0.038																
1	2	1½	C	.036	.132	.016	.68	.56	.457		.65	.46	.517		.54	.40	.642		.44	.38	.560	1.71
1	2	3	C	.097	.153	−.029	1.36	−.06	.456		1.33	−.13	.512		1.05	−.18	.635	1.54	1.01	−.16	.531	.87
1	2	4½	C	.187	.189	−.053	1.61	−.34	.460		1.55	−.39	.517		1.32	−.37	.637	3.60	1.20	−.34	.520	.85
1	3	1½	C	.066			1.32	−.01	.453		1.29	−.08	.511		1.03	−.14	.635	1.49	.98	−.15	.538	.84
1	3	3	C	.156			2.05	−.63	.458		2.00	−.69	.512		1.48	−.52	.623	1.12	1.37	−.49	.494	.66
1	3	4½	C	b.253	.200	−.050																
1	4	1½	C	.081			.92	.19	.457		1.14	−.10	.511	1.88	1.22	−.31	.635	1.92	1.21	−.36	.515	.78
1	4	3	C	b.168			1.39	−.22	.460		1.63	−.51	.515		1.56	−.62	.626	.99	1.46	−.60	.485	.64
1	4	4½	C	b.262			1.68	−.34	.459		1.75	−.53	.511	3.58	1.62	−.69	.626	1.05	1.51	−.66	.475	.60
2	1	1½	C	.081			2.06	−.64	.453		1.75	−.51	.512		1.31	−.29	.628	.60	1.12	−.24	.518	.87
2	1	3	C	.176			2.38	−1.08	.458		2.13	−.95	.514		1.63	−.68	.625	.71	1.44	−.56	.468	.56
2	1	4½	C	.296	.162	−.078	2.53	−1.25	.452	3.59	2.29	−1.11	.511		1.81	−.82	.622	.72	1.54	−.65	.440	.47
2	2	1½	C	.086					.454				.512		1.61	−.65	.634	1.22	1.38	−.54	.438	.40
2	2	3	C	.186			2.80	−1.09	.448	.84	2.60	−1.11	.505	1.08	1.94	−.95	.613	.58	1.61	−.71	.408	.43
2	2	4½	C	b.286	.151	−.017	2.47	−1.12	.451	1.73	2.46	−1.18	.508	1.98	2.05	−1.04	.618	.75	1.64	−.78	.392	.37
2	3	1½	C	.100			1.12	.22	.458		1.38	−.08	.513		1.45	−.46	.626	.63	1.33	−.49	.480	.58
2	3	3	C	b.198			1.61	−.19	.452	1.82	1.79	−.46	.508	1.23	1.77	−.80	.624	.76	1.62	−.74	.431	.48
2	3	4½	C	b.292	−.014	.075	1.88	−.34	.449	.58	1.98	−.61	.506	.86	1.97	−.92	.618	.70	1.64	−.80	.420	.44
1	3	3	D	.156			1.92	−.54	.440		1.77	−.55	.500		1.50	−.51	.613			−.49	.550	
1	1	1½	E	.024			1.25	1.33	.451		1.20	1.10	.511		.50	.66	.632		.38	.58	.583	
1	1	3½	E	.122			2.66	.06	.441		2.05	.01	.500	1.19	1.30	−.09	.613	.47	1.03	−.07	.527	.76
1	1	4½	E	.182	.232	−.040																
1	2	1½	E	.036	.155	.054																
1	2	3	E	.097	.323	−.037																
1	2	4½	E	.187	.338	−.078	4.80	−1.04	.441		3.62	−.90	.500		1.94	−.58	.612	2.15	1.40	−.45	.440	.58
1	3	3	E	.156			4.78	−1.08	.438	5.56	3.67	−.98	.495	1.56	2.08	−.78	.610	1.58			.408	
1	3	4½	E	b.253	.333	−.080																
1	3	d4½	E	b.253	.298	−.064																
2	1	4½	E	.296	.334	−.120			.438		4.31	−1.64	.490	1.82	2.48	−1.16	.588	.92	1.80	−.79	.340	.51
2	1	d4½	E	b.296	.334	−.108	5.15	−2.18	.447		4.04	−1.62	.504	2.28	2.42	−.98	.610	2.28	1.81	−.78	.370	.63
2	2	4½	E	b.286	.393	−.066	6.10	−2.06	.435	3.20	4.63	−1.83	.495	4.57	2.69	−1.31	.582	.89	1.93	−.90	.290	.44
2	3	3	E	.198			5.02	−.87	.437	3.98	4.01	−1.04	.493	2.45	2.53	−1.12	.590	1.00	1.83	−.84	.335	.51

ª η_0.   b Constricted.   c Struts changed.   d With disk.

TABLE I.—CONDENSED EXPERIMENTAL RESULTS—Continued

CONDUCTANCE=0.078

Nose	Slot	Slot opening (in.)	Propeller	A_2/F	$1/\sqrt[3]{P_c}=0$		$1/\sqrt[3]{P_c}=0.5$				$1/\sqrt[3]{P_c}=0.6$				$1/\sqrt[3]{P_c}=1.0$				$1/\sqrt[3]{P_c}=1.6$			
					$\frac{\Delta p}{n^2D^2}\times1000$	$\frac{p_r}{n^2D^2}\times1000$	$\frac{\Delta p}{q}$	$\frac{p_r}{q}$	η_n	η_p	$\frac{\Delta p}{q}$	$\frac{p_r}{q}$	η_n	η_p	$\frac{\Delta p}{q}$	$\frac{p_r}{q}$	η_n	η_p	$\frac{\Delta p}{q}$	$\frac{p_r}{q}$	η_n	η_p
1	1	1½	C	0.024			0	1.19	0.459	0	0.10	0.98	0.517		0.11	0.78	0.649		0.08	0.76	0.600	0.46
1	1	3½	C	.122			1.05	.38	.449	.18	.89	.40	.510	.91	.59	.32	.640	.85	.54	.32	.570	.74
1	1	4½	C	.182	0.108	-0.018					.28	.77	.519		.20	.70	.644		.16	.69	.569	
1	2	1½	C	.036	.022	.051	.23	.88	.458													
1	2	3	C	.097	.058	.025	.92	.43	.452	1.66	.90	.32	.512		.68	.23	.633	1.21	.64	.22	.535	1.05
1	2	4½	C	.187	.152	-.032	1.24	.19	.459		1.19	.03	.515		1.02	-.08	.633	2.22	.99	-.11	.496	.87
1	3	1½	C	.066			.62	.62	.459		.68	.48	.517		.59	.35	.640		.50	.35	.559	3.63
1	3	3	C	.156			1.80	-.06	.460		1.62	-.22	.516		1.13	-.17	.626	1.29	1.04	-.15	.477	.74
1	3	4½	C	[b].253	.119	-.021																
1	4	1½	C	.081			.48	.62	.460		.74	.32	.520		.75	.18	.640		.72	.15	.530	1.08
1	4	3	C	[b].168			.99	.27	.458		1.17	-.04	.515		1.18	-.21	.621	1.01	1.14	-.26	.465	.75
1	4	4½	C	[b].262			1.35	.08	.459		1.39	-.16	.512		1.27	-.35	.627	1.66	1.22	-.32	.439	.66
2	1	1½	C	.081			1.04	.34	.457		.96	.33	.512		.71	.33	.632	.64	.55	.32	.544	1.80
2	1	3	C	.176			1.66	-.31	.458		1.59	-.35	.512		1.32	-.30	.615	.74	1.18	-.28	.468	.88
2	1	4½	C	.296	.086	-.035	2.15	-.70	.451	2.96	1.92	-.64	.508	2.88	1.51	-.52	.605	.70	1.40	-.47	.405	.67
2	2	1½	C	.086			1.30	.14	.453		1.28	.04	.509	2.36	1.04	-.04	.625	.76	.93	-.04	.490	.82
2	2	3	C	.186			2.15	-.58	.448	1.19	1.95	-.58	.503	1.65	1.52	-.51	.611	.80	1.34	-.44	.391	.57
2	2	4½	C	[b].286	.098	-.003	2.16	-.75	.450	1.99	2.00	-.73	.505	2.28	1.65	-.64	.603	.74	1.45	-.54	.351	.52
2	3	1½	C	.100			.65	.64	.457		.88	.32	.514		.91	.17	.631	.87	.87	-.01	.494	.78
2	3	3	C	[b].198			1.19	.20	.452	2.44	1.37	-.07	.507	1.41	1.35	-.35	.620	.91	1.28	-.38	.410	.60
2	3	4½	C	[b].292	-.018	.063	1.64	-.18	.452	3.95	1.65	-.35	.510	6.90	1.51	-.49	.603	.65	1.36	-.45	.384	.56
1	3	3	D	.156			1.44	.06	.440		1.36	-.10	.500		1.12	-.12	.608			-.15	.539	
1	1	1½	E	.024			.52	1.80	.448		.42	1.54	.508		.24	.96	.635		.13	.81	.588	
1	1	3½	E	.122			1.92	.82	.447		1.54	.65	.505		.94	.33	.619	1.26	.68	.30	.526	.87
1	1	4½	E	.182	.172	.019																
1	2	1½	E	.036	.078	.114																
1	2	3	E	.097	.221	.029																
1	2	4½	E	.187	.296	-.039	3.85	-.23	.444		2.97	-.31	.500		1.54	-.30	.604	1.50	1.15	-.17	.403	.90
1	3	3	E	.156			3.97	-.47	.438	8.92	3.01	-.46	.493	5.05	1.67	-.38	.600	1.28	1.18	-.20	.400	.99
1	3	4½	E	[b].253	.288	-.039																
1	3	4½	E	[d][b].253	.273	-.028																
2	1	4½	E	.296	.303	-.073			.438		3.68	-1.29	.490	3.03	2.08	-.78	.582	1.28	1.56	-.54	.312	.74
2	1	4½	E	[d].296	.307	-.081	4.46	-1.14	.445		3.50	-1.00	.503		2.10	-.70	.606	3.02	1.60	-.59	.333	.87
2	2	4½	E	[b].286	.349	-.062	5.23	-1.48	.437	8.90	4.07	-1.42	.492	4.54	2.19	-.92	.562	.93	1.64	-.59	.235	.57
2	3	3	E	[b].198			4.46	-.62	.436	5.26	3.37	-.72	.492	3.42	1.94	-.63	.588	1.34	1.46	-.43	.308	.66

CONDUCTANCE=0.116

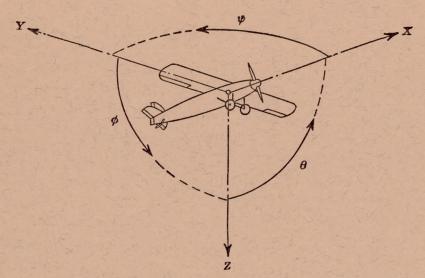| Nose	Slot	Slot opening (in.)	Propeller	A_2/F	$1/\sqrt[3]{P_c}=0$		$1/\sqrt[3]{P_c}=0.5$				$1/\sqrt[3]{P_c}=0.6$				$1/\sqrt[3]{P_c}=1.0$				$1/\sqrt[3]{P_c}=1.6$			
					$\frac{\Delta p}{n^2D^2}\times1000$	$\frac{p_r}{n^2D^2}\times1000$	$\frac{\Delta p}{q}$	$\frac{p_r}{q}$	η_n	η_p	$\frac{\Delta p}{q}$	$\frac{p_r}{q}$	η_n	η_p	$\frac{\Delta p}{q}$	$\frac{p_r}{q}$	η_n	η_p	$\frac{\Delta p}{q}$	$\frac{p_r}{q}$	η_n	η_p
1	1	1½	C	0.024			-0.14	1.35	0.455		0.03	1.12	0.515		0.04	0.83	0.653		0.04	0.81	0.597	0.12
1	1	3½	C	.122			.52	.90	.456	0.26	.42	.74	.511	0.66	.37	.55	.640	0.63	.34	.54	.580	.80
1	1	4½	C	.182	0.036	0.031																
1	2	1½	C	.036	.016	.050	.05	1.04	.457		.10	.91	.515		.13	.79	.643		.07	.76	.570	
1	2	3	C	.097	.083	.017	.42	.70	.453		.54	.60	.514		.44	.50	.640		.38	.50	.545	1.08
1	2	4½	C	.187	.085	.010	.79	.53	.465		.90	.35	.522		.82	.19	.625	1.11	.79	.12	.486	.82
1	3	1½	C	.066			.40	.86	.455		.38	.68	.513		.29	.61	.641		.27	.59	.560	2.59
1	3	3	C	.156			1.32	.46	.457		1.15	.31	.515		.82	.17	.626	1.19	.75	.17	.488	.77
1	3	4½	C	[b].253	.047	.013																
1	4	1½	C	.081			.20	.93	.455		.42	.70	.515		.45	.49	.629	.62	.43	.45	.536	.89
1	4	3	C	[b].168			.61	.58	.460		.80	.32	.519		.88	.13	.620	.93	.85	.06	.462	.70
1	4	4½	C	[b].262			.80	.51	.459		.95	.26	.517		.99	.04	.625	1.48	.93	-.02	.415	.55
2	1	1½	C	.081			.56	.77	.457		.42	.68	.512		.34	.58	.633	3.39	.32	.57	.550	2.08
2	1	3	C	.176			1.05	.28	.460		1.04	.18	.513		.99	.06	.628	1.20	.92	0	.474	.96
2	1	4½	C	.296	.072	-.010	1.56	-.10	.452	5.45	1.56	-.22	.508	3.14	1.37	-.31	.603	.83	1.21	-.30	.401	.83
2	2	1½	C	.086			.91	.52	.453		.86	.44	.511		.68	.34	.630	.79	.59	.33	.516	.99
2	2	3	C	.186			1.72	-.06	.450	2.10	1.57	-.13	.504	1.36	1.22	-.16	.613	.92	1.11	-.16	.390	.64
2	2	4½	C	[b].286	.063	.011	1.65	-.12	.450	1.99	1.67	-.26	.505	1.75	1.49	-.35	.591	.74	1.23	-.32	.343	.58
2	3	1½	C	[b].100			.38	.91	.459		.60	.65	.515		.60	.41	.641	2.08	.56	.34	.512	.84
2	3	3	C	[b].198			.91	.52	.452	2.43	1.08	.26	.508	1.81	1.08	-.01	.616	.84	1.02	-.07	.420	.68
2	3	4½	C	[b].292	-.038	.068	.91	.27	.452	2.43	1.17	.06	.507	1.53	1.22	-.14	.604	.72	1.09	-.17	.377	.57
1	3	3	D	.156			.98	.44	.440		.89	.31	.500		.79	.20	.623		.78	.18	.534	
1	1	1½	E	.024			.33	2.15	.449		.28	1.69	.512		.15	1.02	.636		.08	.86	.585	
1	1	3½	E	.122			1.51	1.46	.443		1.15	1.12	.504		.60	.66	.608	.52	.45	.54	.539	.97
1	1	4½	E	.182	.133	.057																
1	2	1½	E	.036	.017	.133																
1	2	3	E	.097	.128	.085																
1	2	4½	E	.187	.212	.028	3.00	.56	.442		2.20	.39	.498		1.06	.17	.610	4.14	.90	.11	.397	.87
1	3	3	E	.156			2.97	.49	.439	17.10	2.28	.46	.494	6.61	1.17	.38	.602	2.25	.87	.20	.399	.84
1	3	4½	E	[b].253	.202	.026																
1	3	4½	E	[d][b].253	.204	.048																
2	1	4½	E	.296	.218	-.004	3.77	-.36	.436	6.08	2.96	-.45	.489	2.92	1.83	-.48	.578		1.44	-.33	.298	
2	1	4½	E	[d].296	.226	.000	3.82	-.22	.448		3.12	-.38	.503		1.94	-.46	.601		1.41	-.36	.328	
2	2	4½	E	[b].286	.258	-.006	3.75	-.46	.439	24.18	2.97	-.52	.495		1.96	-.53	.563		1.45	-.32	.213	
2	3	3	E	[b].198			3.53	.07	.440		2.65	-.01	.495		1.54	-.15	.585		1.22	-.11	.322	

[a] η_0 [b] Constricted.   [c] Struts changed.   [d] With disk.

Positive directions of axes and angles (forces and moments) are shown by arrows

Axis			Moment about axis			Angle		Velocities	
Designation	Symbol	Force (parallel to axis) symbol	Designation	Symbol	Positive direction	Designation	Symbol	Linear (component along axis)	Angular
Longitudinal	X	X	Rolling	L	$Y \longrightarrow Z$	Roll	ϕ	u	p
Lateral	Y	Y	Pitching	M	$Z \longrightarrow X$	Pitch	θ	v	q
Normal	Z	Z	Yawing	N	$X \longrightarrow Y$	Yaw	ψ	w	r

Absolute coefficients of moment

$$C_l = \frac{L}{qbS} \qquad C_m = \frac{M}{qcS} \qquad C_n = \frac{N}{qbS}$$
$$\text{(rolling)} \qquad \text{(pitching)} \qquad \text{(yawing)}$$

Angle of set of control surface (relative to neutral position), δ. (Indicate surface by proper subscript.)

4. PROPELLER SYMBOLS

D, Diameter

p, Geometric pitch

p/D, Pitch ratio

V', Inflow velocity

V_s, Slipstream velocity

T, Thrust, absolute coefficient $C_T = \dfrac{T}{\rho n^2 D^4}$

Q, Torque, absolute coefficient $C_Q = \dfrac{Q}{\rho n^2 D^5}$

P, Power, absolute coefficient $C_P = \dfrac{P}{\rho n^3 D^5}$

C_s, Speed-power coefficient $= \sqrt[5]{\dfrac{\rho V^5}{P n^2}}$

η, Efficiency

n, Revolutions per second, r.p.s.

Φ, Effective helix angle $= \tan^{-1}\left(\dfrac{V}{2\pi rn}\right)$

5. NUMERICAL RELATIONS

1 hp.=76.04 kg-m/s=550 ft-lb./sec.

1 metric horsepower=1.0132 hp.

1 m.p.h.=0.4470 m.p.s.

1 m.p.s.=2.2369 m.p.h.

1 lb.=0.4536 kg.

1 kg=2.2046 lb.

1 mi.=1,609.35 m=5,280 ft.

1 m=3.2808 ft.